Acknowledgements

We thank P. Ohresser, S. S. Dhesi, K. Larsson and N. B. Brookes of beamline ID12B of the European Synchrotron Radiation Facility in Grenoble for their assistance during the experiment.

Correspondence and requests for materials should be addressed to P.G. (e-mail: pietro.gambardella@epfl.ch).

An ordered mesoporous organosilica hybrid material with a crystal-like wall structure

Shinji Inagaki*, Shiyou Guan*†, Tetsu Ohsuna‡ & Osamu Terasaki§

** Toyota Central R&D Laboratories, Inc., Nagakute, Aichi, 480-1192, Japan*
‡ Institute for Materials Research, Tohoku University, Sendai 980-8577, Japan
§ Department of Physics and CREST, JST, Graduate School of Science, Tohoku University, Sendai 980-8578, Japan
† Present address: Sanyo Chemical Industry, Ltd, Higashiyama, Kyoto, 605-0995, Japan

Surfactant-mediated synthesis strategies are widely used to fabricate ordered mesoporous solids[1–6] in the form of metal oxides[7], metals[8], carbon[9] and hybrid organosilicas[10–14]. These materials have amorphous pore walls, which could limit their practical utility. In the case of mesoporous metal oxides, efforts to crystallize the framework structure by thermal[15,16] and hydrothermal treatments[17] have resulted in crystallization of only a fraction of the pore walls. Here we report the surfactant-mediated synthesis of an ordered benzene–silica hybrid material; this material has an hexagonal array of mesopores with a lattice constant of 52.5 Å, and crystal-like pore walls that exhibit structural periodicity with a spacing of 7.6 Å along the channel direction. The periodic pore

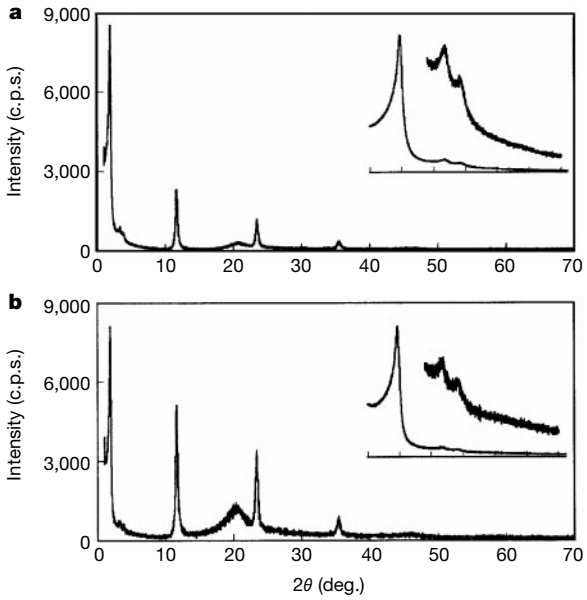

Figure 1 Powder X-ray diffraction patterns of mesoporous benzene–silicas. **a**, Material after removal of surfactants. **b**, As-made material containing surfactants. Patterns in the low-angle region ($1 < 2\theta < 7$) are shown magnified in the insets. These materials have both mesoscale ($d = 45.5$, 26.0 and 22.9 Å) and molecular-scale ($d = 7.6$, 3.8 and 2.5 Å) periodic structures.

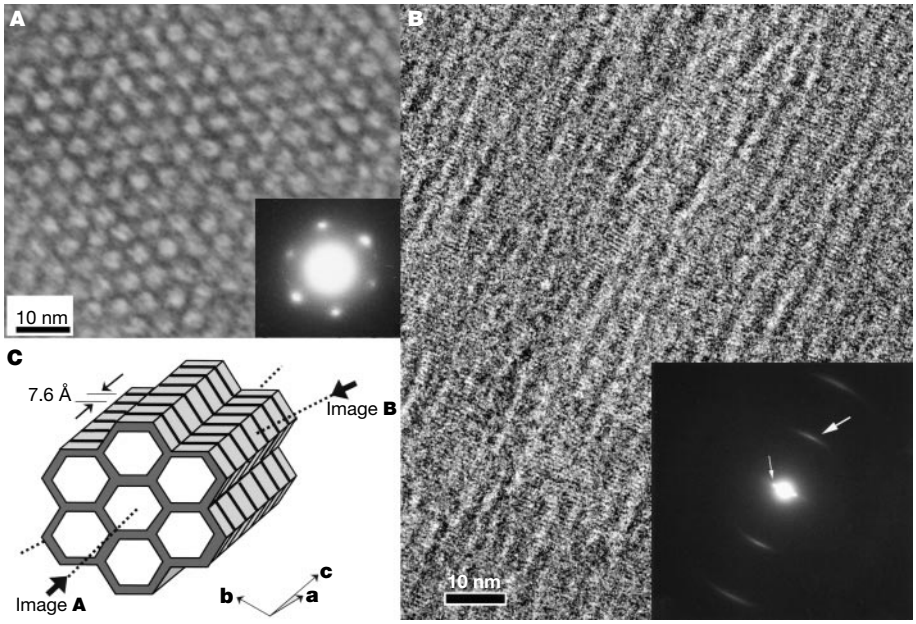

Figure 2 TEM images, electron diffraction patterns and the resulting structural model of mesoporous benzene–silica. The images and the patterns are arranged in the correct orientation relation—that is, the diffraction spots and corresponding lattice planes are normal to each other. **A,** Image and pattern taken with [001] incidence, parallel to the channels. Uniform mesopores with a diameter of 38 Å are arranged in a hexagonal manner. **B,** Image and pattern taken with [100] incidence, perpendicular to the channels. Many lattice fringes with a spacing of 7.6 Å are observed in the pore walls. The wavy contrast, which is perpendicular to the lattice fringes, with a spacing of 45.5 Å ($d = \sqrt{3}a/2$) are also discernible. Note that we cannot observe the contrast of 7.6-Å and 45.5-Å spacings at the best condition simultaneously for both, because the dependence of the contrast transfer function of the objective lens on focus condition is different for both. The electron diffraction pattern also shows diffused spots due to the 7.6-Å periodicity (large arrow) in the perpendicular direction to the spots due to channel arrangement with $d = 45.5$ Å (small arrow). **C**, Schematic model of mesoporous benzene–silica derived from the results of the TEM images and electron diffraction patterns.

surface structure results from alternating hydrophilic and hydrophobic layers, composed of silica and benzene, respectively. We believe that this material is formed as a result of structure-directing interactions between the benzene–silica precursor molecules, and between the precursor molecules and the surfactants. We expect that other organosilicas and organo-metal oxides can be produced in a similar fashion, to yield a range of hierarchically ordered mesoporous solids with molecular-scale pore surface periodicity.

To produce the material, the benzene-bridged organosilane monomer, $(C_2H_5O)_3Si–C_6H_4–Si(OC_2H_5)_3$ (1,4-bis(triethoxysilyl)-benzene, BTEB), was added to an aqueous solution of alkyltrimethylammonium surfactant (3.3 wt%) containing sodium hydroxide, and kept at 95 °C for about 20 hours. It is important to ensure that the solution is alkaline, and the mixture ratio optimized. The benzene–silica hybrid material was obtained by collecting the white precipitate (as-made materials), and removing surfactant by solvent extraction. The material is in the form of plate-like particles (0.5–30 μm in side length and 1 μm in thickness), composed of needle-like single crystals aligned perpendicular to the plate surface (see Supplementary Information).

The powder X-ray diffraction (XRD) pattern of the benzene–silica hybrid material (surfactant-free) showed three peaks in the small-angle scattering regime ($2\theta < 10°$), with spacings d of 45.5, 26.0 and 22.9 Å, which can be indexed to a two-dimensional hexagonal ($p6mm$) lattice with a lattice constant a = 52.5 Å (Fig. 1 a inset). The as-made material, containing surfactant, showed a similar XRD pattern, with the somewhat larger lattice constant a = 53.1 Å (Fig. 1b inset). Both transmission electron microscope (TEM) images and corresponding electron diffraction patterns revealed a clear hexagonal arrangement of one-dimensional channels with uniform size (Fig. 2A and inset). Nitrogen adsorption isotherms also confirmed the existence of uniform mesopores, with the modified BJH (Barrett–Joyner–Halenda) pore diameter[18] of 38 Å. The BET (Brunauer–Emmett–Teller) surface area and mesopore volume were 818 $m^2 g^{-1}$ and 0.66 $cm^3 g^{-1}$, respectively (see Supplementary Information).

The XRD patterns at medium scattering angles (2θ = 10–70°) display four sharp peaks at d = 7.6, 3.8, 2.5 and 1.9 Å (in addition to three peaks at small scattering angles) (Fig. 1a). These diffraction peaks can be explained by a periodic structure with a spacing of 7.6 Å. TEM images reveal many lattice fringes—stacked along the channel axes, with a uniform spacing of 7.6 Å—on the pore walls over the whole region (Fig. 2B). Electron diffraction spots corresponding to 7.6-Å periodicity and its higher order are observed perpendicular to the diffraction spot owing to the mesopore arrangement (with a = 52.5 Å), although we cannot observe higher-order reflections of 45.5-Å periodicity (Fig. 2B inset). These results clearly indicate that molecular-scale periodicity exists in the whole region of the pore walls, which consist of the

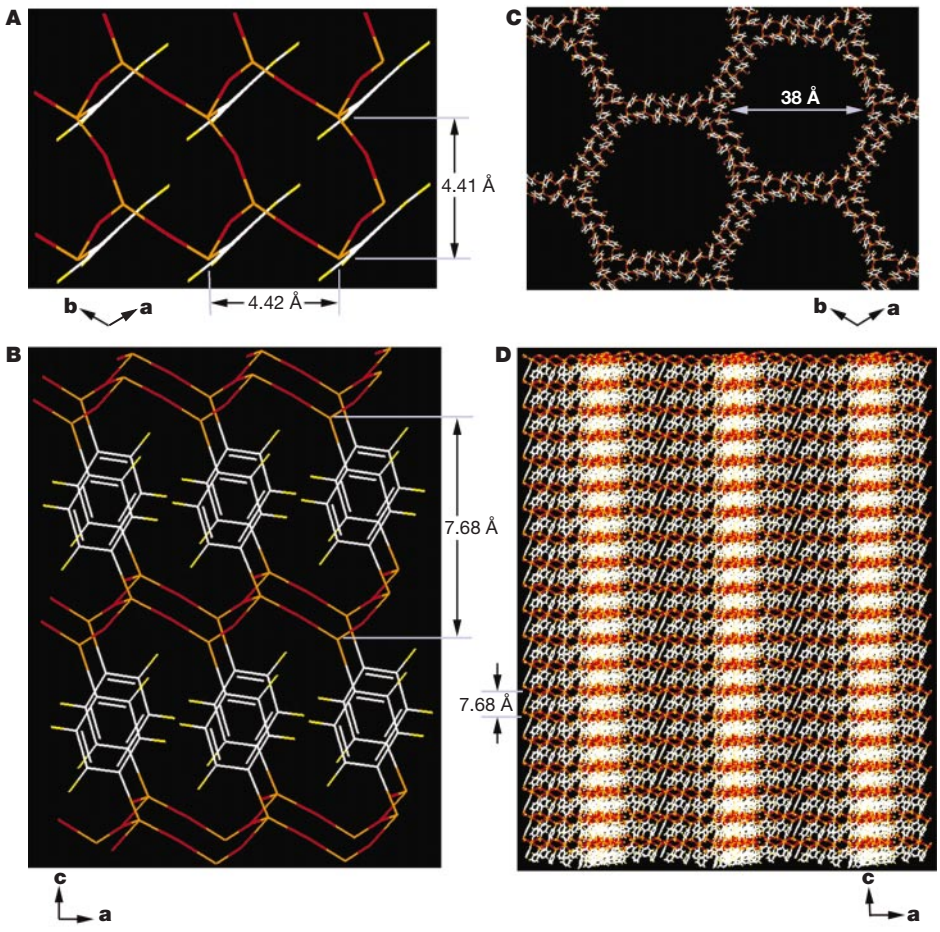

Figure 3 Structural models of mesoporous benzene–silica. **A, B**, Images of the layered arrangement of $SiO_{1.5}–C_6H_4–SiO_{1.5}$ units in the walls. The structure was optimized by minimizing the three-dimensional periodic lattice using the force field COMPASS. **C**, **D**, Images of the hexagonal lattice constructed with the layered pore-wall structure. The structure was also minimized by using the force field COMPASS. Atoms are represented as a stick model. Silicon, orange; oxygen, red; carbon, white; hydrogen, yellow.

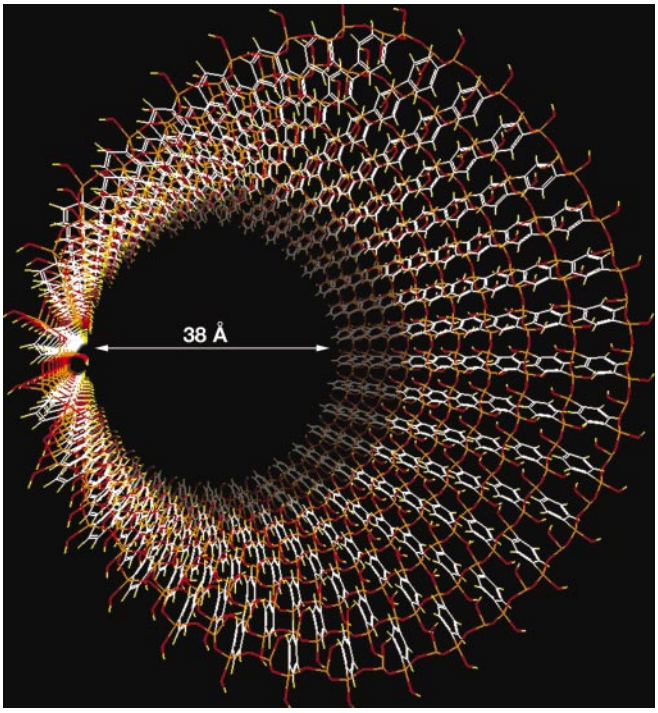

Figure 4 Model showing the pore surface of mesoporous benzene–silica. Benzene rings are aligned in a circle around the pore, fixed at both sides by silicate chains. The silicate is terminated by silanol (Si–OH) at the surface. Hydrophobic benzene layers and hydrophilic silicate layers array alternately at an interval of 7.6 Å along the channel direction. Silicon, orange; oxygen, red; carbon, white; hydrogen, yellow.

benzene–silica composite. As-made mesoporous benzene–silica also displays the 7.6-Å periodicity along the walls (Fig. 2C). The peak intensity of the 7.6-Å periodicity in the powder XRD pattern is almost the same for surfactant-free and as-made mesoporous benzene–silicas, indicating that the periodicity is completely retained after removal of surfactant (Fig. 1b). ^{29}Si and ^{13}C magic angle spinning nuclear magnetic resonance (MAS NMR) measurements clearly showed that the pore walls of the mesoporous benzene–silica are made of a covalently bonded network composed of $O_{1.5}Si–C_6H_4–SiO_{1.5}$ units, and that no carbon–silicon bond cleavage of the BTEB molecule occurred during the synthesis (Supplementary Information). The sharp signals due to silicon species of the ^{29}Si MAS NMR spectra are indicative of a unique and uniform environment around Si atoms in the walls, consistent with the crystal-like pore-wall structure found in XRD, electron diffraction and TEM observations.

Figure 3 shows a structural model of the mesoporous benzene–silica, which is constructed on the basis of the well-defined structure of crystalline 1,4-bis(trihydroxysilyl)benzene ($(HO)_3Si–C_6H_4–Si(OH)_3$, BTHB; ref. 19). The BTHB molecule, a triol analogue of the BTEB molecule, forms a layered structure in which BTHB molecules are packed in a head-to-tail manner within sheets with an interlayer spacing of 10.1 Å. Hydrogen-bonding of silanols (Si–OH···HO–Si) among BTHB molecules stabilizes the crystal structure. We substituted covalent bonds (Si–O–Si) for the hydrogen bonds in the model of mesoporous benzene–silica (Fig. 3A and B). Minimizing the framework energy of the covalently bonded periodic lattice using a molecular mechanics simulation resulted in a slight decrease in the interlayer spacing, to 7.68 Å, in good agreement with the 7.6-Å periodicity observed by XRD and electron diffraction patterns. We have constructed a hexagonal lattice model of the mesoporous structure on the basis of the periodic pore-wall structure (Fig. 3C and D). The side view of the pore walls in the model (Fig. 3D) resembles very closely the images of TEM (Fig. 2B), supporting the validity of the structural model. The mesoporous benzene–silica is thus a hierarchically ordered porous material, displaying both meso- and molecular-scale periodicity. The material had extremely high thermal and hydrothermal stability: thermogravimetric analysis showed that benzene groups were kept in the walls up to 500 °C in air or nitrogen (Supplementary Information), and the meso-and molecular-scale periodicity was completely preserved even after boiling the material in water for 8 hours.

Self-assembly of the framework source of organosilane BTEB molecules formed the periodic structure in the walls of the mesoporous benzene–silica probably because hydrophobic and hydrophilic interactions directed the self-assembly of BTEB molecules into the framework structure[19]. Similar molecular-scale periodicity was also observed in mesoporous ethylene (–CH = CH–)–silica, though it had smaller molecular-scale periodicity (5.6 Å). The periodicity in the walls increased with increasing molecular length of organic groups, suggesting that the layered structure with the organic group as a pillar is essential for formation of the organosilica hybrid materials. In the case of smaller interactive organic groups of ethane ($–CH_2–CH_2–$) and methane ($–CH_2–$), the mesoporous materials showed no molecular-scale periodicity, even though they had highly ordered mesostructures. This suggests that strong interaction of organosilane molecules is important to form the molecular-scale ordered structures. However, molecular-scale periodicity is not seen in the non-periodic amorphous benzene–silica and other organic–inorganic hybrid materials produced by sol–gel methods not using surfactants[20,21]. This suggests that the self-assembly of the surfactant and the resulting mesostructure promotes the formation of the molecular-scale periodic wall structure. These observations suggest that analogous interactions can be exploited in the synthesis of a variety of hierarchically ordered materials with not only hybrid organosilicas but also hybrid organo–metal oxides.

We find a unique surface structure in the model of mesoporous benzene–silica, in which hydrophilic silicate layers and hydrophobic benzene layers array alternately (Fig. 4). This structure, with periodically arranged hydrophobic–hydrophilic surfaces, could enable structural orientation of guest molecules or clusters enclosed in the pores, which in turn might improve the selectivity and activity in catalytic applications, and enhance the opto-electrical efficiency of included molecules and clusters. We have sulphonated the mesoporous benzene–silica while preserving both the meso- and molecular-scale ordered structures (see Supplementary Information). The sulphonic acid-functionalized mesoporous material might find use as a solid acid catalyst that can be readily recovered and reused[22]. The sulphonate groups were kept at pore walls up to 500 °C in air or nitrogen, as confirmed by mass spectroscopy. This unusually high thermal stability would allow the use of this solid acid catalyst not only in liquid-phase reactions, but also in gas-phase reactions at high temperature. Because the sulphonic acid groups serve as carriers of protons, the sulphonated mesoporous benzene–silica might also find use as an electrolyte for fuel cells. Moreover, fluorescence spectra indicate some interactions between benzene rings in the walls (see Supplementary Information). The closest intermolecular distance of benzene rings is 4.4 Å in the model (Fig. 3A); if closer staking of benzene rings in the walls could be achieved, π–π conjugation of the rings would render the porous framework conducting. □

Methods

Preparation of mesoporous benzene–silica material

Mesoporous benzene–silica was synthesized from 1,4-bis(triethoxysilyl)benzene (BTEB), Azmax Japan, in the presence of octadecyltrimethylammonium chloride (ODTMA) surfactant. ODTMA (16.665 g, 47.88 mmol) was dissolved in a mixture of ion-exchanged water (500 g) and 6 M sodium hydroxide (NaOH) aqueous solution (40 g, 200 mmol NaOH) at 50–60 °C. BTME (20 g, 49.67 mmol) was added to the ODTMA solution under vigorous stirring at room temperature. The mixture was treated ultrasonically for 20 min

to disperse the hydrophobic BTEB in the aqueous solution, and stirred for 20 h at room temperature. The solution was kept at 95 °C for 20 h under static conditions. The resulting white precipitate was recovered by filtration and drying to yield as-made mesoporous benzene–silica material (8.22 g). Surfactant was removed by stirring 1.0 g of as-synthesized material in 250 ml of ethanol with 9 g of 36% HCl aqueous solution at 70 °C for 8 h to yield mesoporous benzene–silica (0.69 g).

Sulphonation of mesoporous benzene–silica

The mesoporous benzene–silica was dried under evacuation at 10^{-2}–10^{-3} torr for 4 h and added to 25% SO_3/H_2SO_4 solution. The dispersed solution was kept at 105–110 °C for 5 h. The dispersion was cooled at room temperature, and added to a large volume of water. The solid was filtered and washed with water repeatedly, then boiled in ion-exchanged water for 1 h, filtered and washed with boiling water repeatedly. Finally, the solid was stirred in 6 M hydrochloric acid aqueous solution for 24 h to protonate and form sulphonic acid groups. The acid content of the mesoporous material was determined from the titration curve. The sulphonated sample (50 mg) was immersed in 10 wt% sodium chloride aqueous solution for 24 h. The solution was titrated with 0.05 M NaOH to produce the titration curve. The acid amount was determined to be 0.40 mequiv. g^{-1}. The sulphonation conditions could sulphonate both the benzene rings and the silica.

Received 1 November 2001; accepted 22 January 2002.

1. Yanagisawa, T., Shimizu, T., Kuroda, K. & Kato, C. The preparation of alkyltrimethylammonium-kanemite complexes and their conversion to microporous materials. *Bull. Chem. Soc. Jpn* **63,** 988–992 (1990).
2. Kresge, C. T., Leonowicz, M. E., Roth, W. J., Vartuli, J. C. & Beck, J. S. Ordered mesoporous molecular sieves synthesized by a liquid-crystal template mechanism. *Nature* **359,** 710–712 (1992).
3. Beck, J. S. *et al.* A new family of mesoporous molecular sieves prepared with liquid crystal templates. *J. Am. Chem. Soc.* **114,** 10834–10843 (1992).
4. Inagaki, S., Fukushima, Y. & Kuroda, K. Synthesis of highly ordered mesoporous materials from a layered polysilicate. *J. Chem. Soc. Chem. Commun.* 680–682 (1993).
5. Firouzi, A. *et al.* Cooperative organization of inorganic-surfactant and biomimetic assemblies. *Science* **267,** 1138–1143 (1995).
6. Bagshaw, S. A., Prouzet, E. & Pinnavaia, T. J. Templating of mesoporous molecular sieves by nonionic polyethylene oxide surfactants. *Science* **269,** 1242–1244 (1995).
7. Ying, J. Y., Mehnert, C. P. & Wong, M. S. Synthesis and applications of supramolecular-templated mesoporous materials. *Angew. Chem. Int. Edn Engl.* **38,** 56–77 (1999).
8. Attard, G. S. *et al.* Mesoporous platinum films from lyotropic liquid crystalline phases. *Science* **278,** 838–840 (1997).
9. Joo, S. H. *et al.* Ordered nanoporous arrays of carbon supporting high dispersions of platinum nanoparticles. *Nature* **412,** 169–172 (2001).
10. Inagaki, S., Guan, S., Fukushima, Y., Ohsuna, T. & Terasaki, O. Novel mesoporous materials with a uniform distribution of organic groups and inorganic oxide in their framework. *J. Am. Chem. Soc.* **121,** 9611–9614 (1999).
11. Melda, B. J., Holland, B. T., Blanford, C. F. & Stein, A. Mesoporous sieves with unified hybrid inorganic/organic framework. *Chem. Mater.* **11,** 3302–3308 (1999).
12. Asefa, T., MacLachlan, M. J., Coombs, N. & Ozin, G. A. Periodic mesoporous organosilicas with organic groups inside the channel walls. *Nature* **402,** 867–871 (1999).
13. Guan, S., Inagaki, S., Ohsuna, T. & Terasaki, O. Cubic hybrid organic-inorganic mesoporous crystal with a decaoctahedral shape. *J. Am. Chem. Soc.* **122,** 5660–5661 (2000).
14. Stein, A., Melde, B. J. & Schroden, R. C. Hybrid inorganic-organic mesoporous silicates—Nanoscopic reactors coming of age. *Adv. Mater.* **12,** 1403–1419 (2000).
15. Yang, P., Zhao, D., Margolese, D. I., Chmelka, B. F. & Stucky, G. D. Generalized syntheses of large-pore mesoporous metal oxides with semicrystalline frameworks. *Nature* **396,** 152–155 (1998).
16. Lee, B., Lu, D., Kondo, J. N. & Domen, K. Single crystal particles of a mesoporous mixed transition metal oxide with a wormhole structure. *Chem. Commun.* 2118–2119 (2001).
17. Liu, Y., Zhang, W. & Pinnavaia, T. J. Steam-stable MSU-S aluminosilicate mesostructures assembled from zeolite ZSM-5 and zeolite beta seeds. *Angew. Chem. Int. Edn Engl.* **40,** 1255–1258 (2001).
18. Kruk, M. & Jaroniec, M. Gas adsorption characterization of ordered organic-inorganic nanocomposite materials. *Chem. Mater.* **13,** 3169–3183 (2001).
19. Cerveau, G., Corriu, R. J., Dabiens, B. & Bideau, J. L. Synthesis of stable organo(bis-silanetriols): X-ray powder structure of 1,4-bis(trihydroxysilyl)benzene. *Angew. Chem. Int. Edn Engl.* **39,** 4533–4537 (2000).
20. Loy, D. A. & Shea, K. J. Bridged polysilsesquioxanes—Highly porous hybrid organic-inorganic materials. *Chem. Rev.* **95,** 1431–1442 (1995).
21. Corriu, R. J. P. Ceramics and nanostructures from molecular precursors. *Angew. Chem. Int. Edn Engl.* **39,** 1376–1398 (2000).
22. Harmer, M. A., Farneth, W. E. & Sun, Q. Towards the sulfuric acid of solids. *Adv. Mater.* **10,** 1255–1257 (1998).

Supplementary Information accompanies the paper on *Nature*'s website (http://www.nature.com).

Acknowledgements

We thank S. Yamamoto for help in computer simulation of structural models, and S. Hyde for critical reading of the manuscript. O.T. was supported by CREST, Japan Science and Technology Corporation.

Competing interests statement

The authors declare that they have no competing financial interests.

Correspondence and requests for materials should be addressed to S.I. (e-mail: inagaki@mosk.tytlabs.co.jp).

Origin and fate of Lake Vostok water frozen to the base of the East Antarctic ice sheet

Robin E. Bell*, Michael Studinger*, Anahita A. Tikku*, Garry K.C. Clarke†, Michael M. Gutner*‡ & Chuck Meertens§

* *Lamont-Doherty Earth Observatory, Columbia University, Palisades, New York 10964, USA*
† *Department of Earth and Ocean Sciences, University of British Columbia, Vancouver, BC V6T 1Z4, Canada*
‡ *Department of Geology and Geophysics, Yale University, New Haven, Connecticut 06511, USA*
§ *UNAVCO/UCAR Facility, Boulder, Colorado 80307, USA*

The subglacial Lake Vostok may be a unique reservoir of genetic material and it may contain organisms with distinct adaptations[1–3], but it has yet to be explored directly. The lake and the overlying ice sheet are closely linked, as the ice-sheet thickness drives the lake circulation, while melting and freezing at the ice-sheet base will control the flux of water, biota and sediment through the lake[4–7]. Here we present a reconstruction of the ice flow trajectories for the Vostok core site, using ice-penetrating

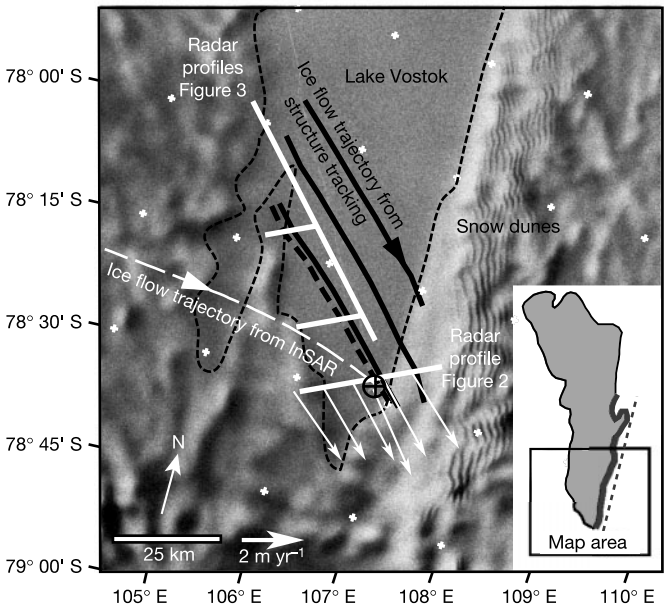

Figure 1 RADARSAT synthetic aperture radar image[15] of the ice sheet surface over the southern part of Lake Vostok. Inset, map showing the outline of the entire lake, indicating the location of the enlarged ice-surface image. In the inset, the heavy line is the region where accreted ice is observed leaving the lake, and the dashed line is the downslope line where the ice flux is estimated. In the RADARSAT image, the grounding line is marked by the fine dashed line between the smooth, featureless ice surface over the lake and the rough ice surface over the grounded ice sheet. The shallow, narrow embayment and its possible connection to the main lake are seen along the western shoreline. The ice flow trajectory shown white is derived from interferometry[4,12]. The four ice flow trajectories derived from internal layer structures are shown as black lines across the lake. The Vostok flow trajectory is illustrated as a dashed black line. The Vostok ice-core site is marked by the circle. The location of the radar profile shown in Fig. 2 is indicated by the long white line that crosses the Vostok core site. The radar profiles shown in the 'fence diagram' (Fig. 3) are shown as the intersecting white lines to the northwest. The GPS velocity vectors are shown as arrows.